Travelling waves in arrays of delay-coupled phase oscillators

Carlo R. Laing*
Institute of Natural and Mathematical Sciences, Massey University, Private Bag 102-904 NSMC, Auckland, New Zealand
(Dated: April 1, 2016)

We consider the effects of several forms of delays on the existence and stability of travelling waves in non-locally coupled networks of Kuramoto-type phase oscillators, and theta neurons. By passing to the continuum limit and using the Ott/Antonsen ansatz we derive evolution equations for a spatially-dependent order parameter. For phase oscillator networks the travelling waves take the form of uniformly twisted waves, and these can often be characterised analytically. For networks of theta neurons, the waves are studied numerically.

PACS numbers: 05.45.Xt
Keywords: phase oscillators, Ott/Antonsen, travelling waves, delays, Kuramoto, theta neuron

One of the simplest forms of behaviour of an array of coupled oscillators is a travelling wave with constant speed. Here we consider two types of non-locally coupled networks of heterogeneous phase oscillators which show travelling wave solutions, and investigate the effects of including different forms of delays in their coupling. By taking the continuum limit and using the Ott/Antonsen ansatz we derive evolution equations for a spatially-dependent order parameter. Numerical and bifurcation analysis of these equations gives results on the existence and stability of travelling waves, and their dependence on delays.

I. INTRODUCTION

The study of networks of coupled oscillators has a long history and encompasses many different areas of science [49]. One particular type of network of interest is an array, or lattice, of oscillators [17, 26, 27, 31, 35, 45], which can be thought of as a discretisation of a continuous oscillatory medium. A common simplification when studying networks of coupled oscillators is to describe the state of an oscillator by a single variable, its phase [52]. This simplification is valid when oscillators are weakly coupled, for example [15, 16]. One type of solution which can occur in an array of non-locally coupled oscillators is the chimera state [30, 48] in which some oscillators are synchronised while the remainder are asynchronous. Another simpler type of solution is a travelling wave, described by a fixed profile which travels at a constant speed. Such waves have been observed in various neural systems [16, 23, 50, 51] and are often associated with pathological states such as cortical spreading depression and epileptic seizures [5]. One particular type of travelling wave is a uniformly twisted state in which, at any moment in time, the phase of oscillators varies linearly with spatial position [21, 41]. Such states have been previously studied in networks of identical oscillators [59] and later in heterogeneous networks [45].

Delayed interactions between different nodes in a network often occur. One example is a transmission delay, in which a signal propagates (along a neuron's axon, for example) at a constant speed, and thus the delay is proportional to the distance between units [7, 53, 63]. Another example is a fixed delay [9, 43, 62], representing the time taken for certain processes to occur, for example the kinetics of synaptic transmission between two neurons [8, 16], or the passage of light through a laser [36]. A third possibility involves distributed delays [2, 38, 39], which may result from there being many connections between two nodes, with different delays along each path. A related concept is that of distributed transmission velocities [3]. One may also consider systems simultaneously possessing two or more of these types of delays [18].

In this paper we investigate the effects of including various types of delay on the existence and stability of both uniformly twisted waves in a network of Kuramoto oscillators, and travelling waves in a network of theta neurons, to better understand the effects of delays on such types of waves.

*Electronic address: c.r.laing@massey.ac.nz

In both networks we assume that the oscillators are heterogeneous. The effects of delays on the dynamics of coupled oscillator networks have been considered a number of times previously [10, 15, 24, 52, 55], but here we will extensively use the recent ansatz of Ott and Antonsen [46, 47] to derive continuum level descriptions of travelling waves, which will make the formulation of delayed equations straightforward.

We study Kuramoto oscillators in Sec. II and theta neurons in Sec. III. For the Kuramoto oscillators we consider constant delays in Sec. II B, transmission delays in Sec. II C and distributed delays in Sec. II D. For the theta neurons we consider only distributed delays, in Sec. III C.

II. KURAMOTO OSCILLATORS

We first consider a network of Kuramoto oscillators, i.e. non-identical phase oscillators coupled by a sinusoidal function of phase differences [1, 28, 57].

A. Theory

The model consists of N phase oscillators on a one-dimensional lattice, each coupled to $M \in \mathbb{Z}^+$ neighbours either side:

$$\frac{d\theta_j}{dt} = \omega_j + \frac{K}{2M+1} \sum_{k=-M}^{M} \sin\left(\theta_{j+k} - \theta_j\right) \tag{1}$$

for $j = 1, 2 \ldots N$, where periodic boundary conditions in index (space) are taken and K is the coupling strength. We assume that the ω_j are randomly chosen from a Lorentzian distribution, $g(\omega)$, with mean Ω_0 and half-width-at-half-maximum 1, i.e.

$$g(\omega) = \frac{1/\pi}{(\omega - \Omega_0)^2 + 1} \tag{2}$$

This type of model has been studied previously [44, 60] and the presentation here follows [45]. (The authors [45] actually considered the more general case, where $\theta_{j+k} - \theta_j$ in (1) was replaced by $\theta_{j+k} - \theta_j - \alpha$ for some constant α.) The choice of a Lorentzian for $g(\omega)$ is common [30, 31, 38, 39, 45–47], and allows one to analytically evaluate an integral in (11) (below), although it is not clear that all results for a Lorentzian apply when other similar distributions are used [29]. Note that the dynamics of (1) depend on only phase differences, i.e. the system is invariant under a uniform phase shift: $\theta_j \mapsto \theta_j + \gamma$ for all j, where γ is an arbitrary constant.

Defining a complex mean field at each lattice point by

$$Z_j(t) = \frac{1}{2M+1} \sum_{k=-M}^{M} e^{i\theta_{j+k}} \tag{3}$$

we have

$$\frac{d\theta_j}{dt} = \omega_j + K\mathrm{Im}\left[Z_j e^{-i\theta_j}\right] = \omega_j + \frac{K}{2i}\left[Z_j e^{-i\theta_j} - \overline{Z}_j e^{i\theta_j}\right] \tag{4}$$

where overbar indicates complex conjugate. We fix the length of the periodic domain to be 2π so that oscillator j is at spatial position $x_j = 2\pi j/N$ and take the continuum limit $N, M \to \infty$ in such a way that $M/N \to \sigma < 1/2$. The system is then described by a probability density function $f(\theta, \omega, x, t)$ such that the probability that an oscillator in $[x, x + dx]$ and with natural frequency in $[\omega, \omega + d\omega]$ has phase in $[\theta, \theta + d\theta]$ at time t is $f(\theta, \omega, x, t)dxd\omega d\theta$, where x is now position along a line segment of length 2π. The continuous analogue of the mean field Z_j is then

$$Z(x,t) = \int_0^{2\pi} G(x-y) \int_{-\infty}^{\infty} \int_0^{2\pi} f(\theta, \omega, y, t) e^{i\theta} d\theta \; d\omega \; dy \tag{5}$$

where

$$G(x) = \begin{cases} \frac{1}{4\pi\sigma}, & |x| < 2\pi\sigma \\ 0, & \text{otherwise} \end{cases} \tag{6}$$

and the spatial integral is evaluated using periodic boundary conditions. The density f satisfies the continuity equation

$$\frac{\partial f}{\partial t} + \frac{\partial}{\partial \theta}(fv) = 0 \tag{7}$$

where

$$v = \omega + \frac{K}{2i}\left[Ze^{-i\theta} - \overline{Z}e^{i\theta}\right] \tag{8}$$

The system (7)-(8) is amenable to the Ott/Antonsen ansatz [46, 47] so we write

$$f(\theta, \omega, x, t) = \frac{g(\omega)}{2\pi}\left[1 + \sum_{n=1}^{\infty}\{\bar{z}(\omega, x, t)\}^n e^{in\theta} + \text{c.c.}\right] \tag{9}$$

for some function $z(\omega, x, t)$ where "c.c." is the complex conjugate of the previous term. This ansatz is an assumption that f takes the particular form (9). Substituting (9) into (5) and (7)-(8) we find that z satisfies

$$\frac{\partial z}{\partial t} = i\omega z + \frac{K}{2}\left[Z - \overline{Z}z^2\right] \tag{10}$$

where

$$Z(x, t) = \int_0^{2\pi} G(x - y)\int_{-\infty}^{\infty} g(\omega)z(\omega, y, t)d\omega\ dy \tag{11}$$

Using contour integration to evaluate the integral over ω in (11) and defining $u(x, t) = z(\Omega_0 - i, x, t)$ we find that u satisfies

$$\frac{\partial u}{\partial t} = (-1 + i\Omega_0)u + \frac{K}{2}\left[Z - \overline{Z}u^2\right] \tag{12}$$

where

$$Z(x, t) = \int_0^{2\pi} G(x - y)u(y, t)dy \tag{13}$$

Partially coherent uniformly-twisted states are solutions of (12)-(13) of the form $u(x, t) = ae^{i(qx+\nu t)}$ where a and ν are real and q is an integer (the "twist" of a twisted state; an integer because of the periodic boundary conditions of the domain). The quantity a $(0 < a < 1)$ measures the coherence level of a state: a increases as the coherence increases, q gives the rate at which the phase of u changes with x at a fixed t, while ν gives the temporal rotation rate of a twisted state. Substituting this form of solution into (12)-(13) we find

$$i\nu = -1 + i\Omega_0 + \frac{K\widehat{G}(q)}{2}(1 - a^2) \tag{14}$$

where $\widehat{G}$ is the Fourier transform of G:

$$\widehat{G}(q) = \int_0^{2\pi} G(x)\cos(qx)dx = \frac{\sin(2\pi\sigma q)}{2\pi\sigma q} \tag{15}$$

for the coupling function given by (6). Equating real and imaginary parts of (14) we find

$$a^2 = 1 - \frac{2}{K\widehat{G}(q)} \qquad \text{and} \qquad \nu = \Omega_0 \tag{16}$$

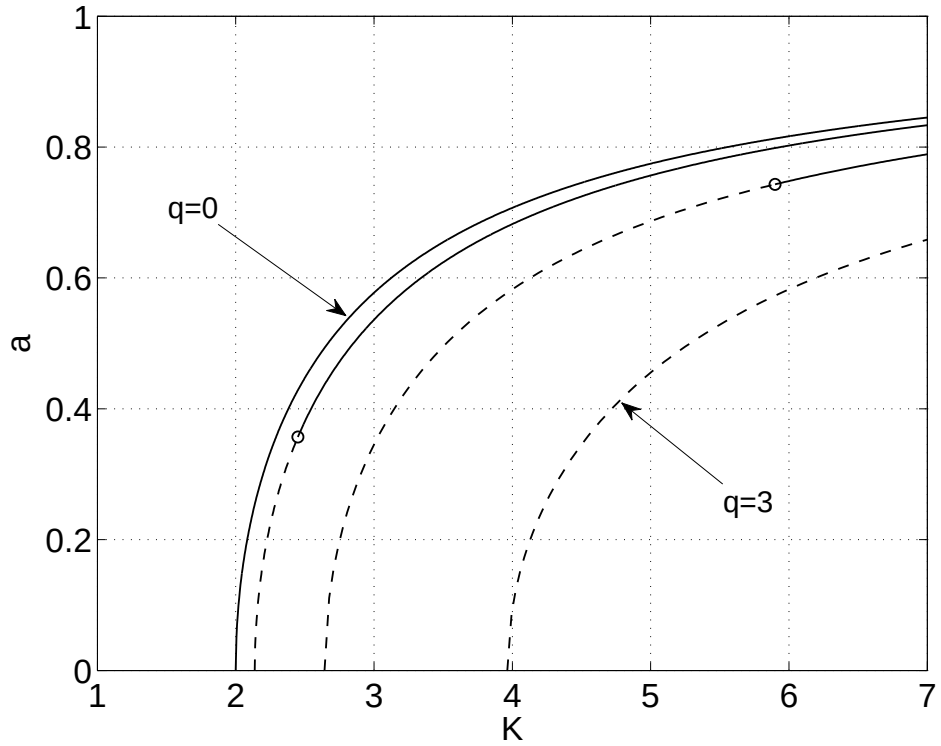

FIG. 1: Twisted state solutions of (12)-(13) with $q = 0, 1, 2, 3$ (top to bottom). Solid: stable; dashed: unstable. The circles indicate Hopf bifurcations. Parameters: $\sigma = 0.1$.

Thus a twisted state with twist q is created as K increases through $2/\widehat{G}(q)$, and the value of Ω_0 is largely irrelevant, as it just sets the rotation rate ν.

The stability of the uniformly incoherent state (corresponding to $u = 0$ in (12)) and of a twisted state can be found analytically by linearising (12)-(13) about them [45], and we do not present the analysis here. The uniformly incoherent state becomes unstable to a perturbation with twist q at the same value of K at which the q-twisted state is created. The 0-twisted state is stable upon creation as K is increased, but the states with higher values of q are unstable when they are created, only stabilising through a subcritical Hopf bifurcation as K is increased further, as shown in Fig. 1. This scenario has similarities to the Eckhaus instability [45, 58].

Figure 2 shows snapshots of twisted waves with $q = 0, 1$ for the original system of phase oscillators (1) at $K = 5$. We see from Fig. 1 that for this value of K these are the only stable twisted states. (All computations were performed using Matlab. Numerical integration was done with `ode45` using default tolerances and continuation using pseudo-arclength methods [33].)

B. Constant delay

We now consider including a constant delay, modelling some sort of "event" of fixed duration which occurs before the influence of an oscillator can be felt by those to which it is connected. We thus modify (1) to

$$\frac{d\theta_j(t)}{dt} = \omega_j + \frac{K}{2M+1}\sum_{k=-M}^{M}\sin\left(\theta_{j+k}(t-\tau) - \theta_j(t)\right) \tag{17}$$

where $\tau \in \mathbb{R}^+$. This can be thought of as a spatially-extended version of [62]. Defining the complex mean field as in (3), moving to the continuum limit and performing the integrals as in Sec. II A we

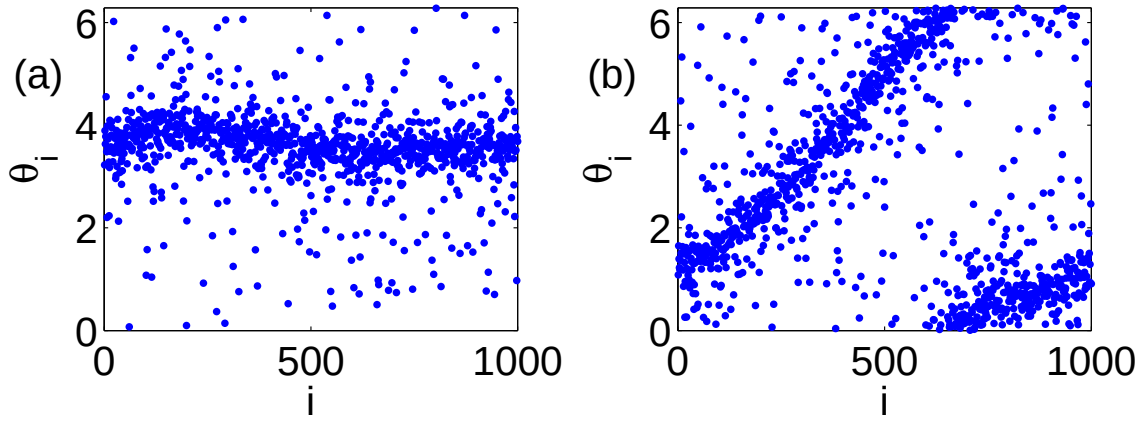

FIG. 2: Snapshots of twisted state solutions of (1) with $q = 0$ (a) and $q = 1$ (b), after transients have been discarded. Initial conditions of $\theta_i(0) = 2\pi qi/N$ were used. Parameters: $N = 1000, M = 100, K = 5, \Omega_0 = 0$.

find that the dynamics are given by

$$\frac{\partial u(x,t)}{\partial t} = (-1 + i\Omega_0)u(x,t) + \frac{K}{2}\left[Z(x,t-\tau) - \overline{Z}(x,t-\tau)u^2(x,t)\right] \tag{18}$$

where $Z(x,t)$ is given by (13). Again looking for solutions of the form $u(x,t) = ae^{i(qx+\nu t)}$ we find that

$$i\nu = -1 + i\Omega_0 + \frac{K\widehat{G}(q)}{2}\left[e^{-i\nu\tau} - a^2 e^{i\nu\tau}\right] \tag{19}$$

and rearranging we find that

$$a^2 = 1 - \frac{2}{K\widehat{G}(q)\cos(\nu\tau)} \tag{20}$$

where ν satisfies

$$\nu = \Omega_0 + \tan(\nu\tau) - K\widehat{G}(q)\sin(\nu\tau) \tag{21}$$

A twisted wave is created when $a = 0$, i.e. when ν satisfies

$$\nu = \Omega_0 - \tan(\nu\tau) \tag{22}$$

Eqn. (22) has an infinite number of solutions for fixed Ω_0 and τ but we will numerically follow the solution branch $\nu(\tau)$ for which $\nu(0) = \Omega_0$, as τ is increased. Substituting this branch into (20) and setting $a = 0$ we can find the value of K at which a q-twisted state is created for a range of τ values. These are shown with solid curves in Fig. 3. As in Sec. II A, the $q = 0$ state is stable upon creation, but the states with higher values of q are unstable upon creation and are stabilised through Hopf bifurcations as K is increased further. To find these Hopf bifurcations we move to a coordinate system rotating at speed ν, i.e. let $\tilde{u}(x,t) = u(x,t)e^{-i\nu t}$ so that $\tilde{u}$ is a fixed point of

$$\frac{\partial \tilde{u}(x,t)}{\partial t} = [-1 + i(\Omega_0 - \nu)]\tilde{u}(x,t) + \frac{K}{2}\left[e^{-i\nu\tau}\widetilde{Z}(x,t-\tau) - e^{i\nu\tau}\overline{\widetilde{Z}}(x,t-\tau)\tilde{u}^2(x,t)\right] \tag{23}$$

where

$$\widetilde{Z}(x,t) = \int_0^{2\pi} G(x-y)\tilde{u}(y,t)dy \tag{24}$$

We then spatially discretise (23)-(24) and follow the fixed points using DDE-BIFTOOL [11] and determine their stability. Several curves of Hopf bifurcations are shown (dashed) in Fig. 3. We see that increasing the delay τ causes all bifurcations to move to higher values of K (for these values of Ω_0 and σ).

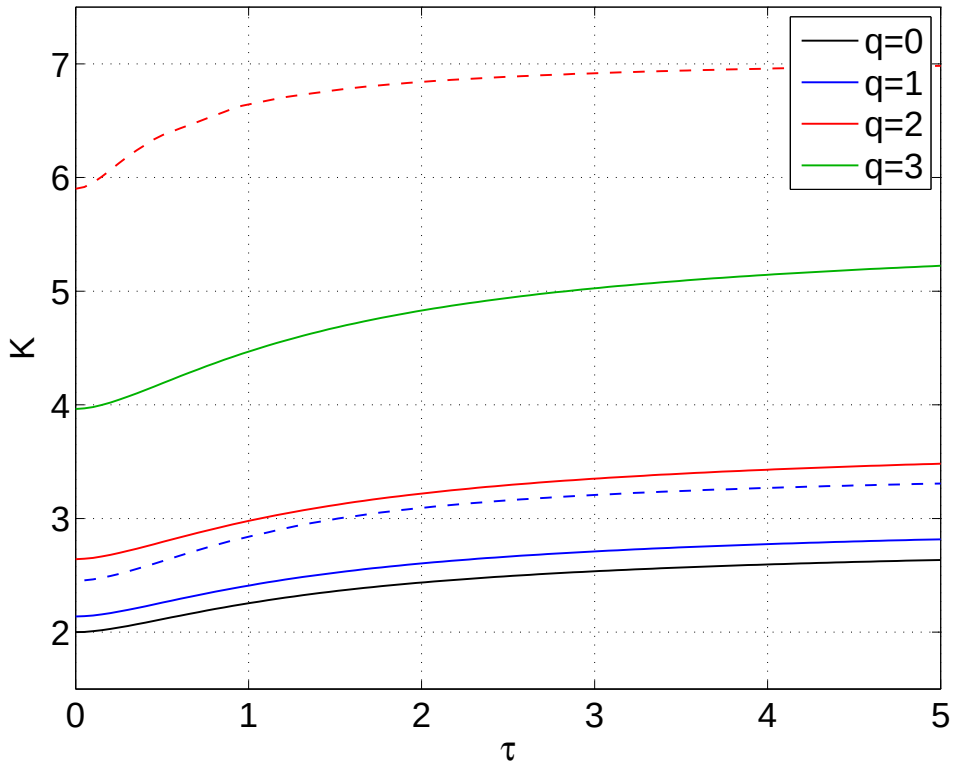

FIG. 3: q-twisted states for constant delay τ are created as the corresponding solid line is crossed from below, and become stable as the dashed line of the same colour is crossed from below. The $q = 0$ state is stable upon creation and the $q = 3$ state is stabilised at higher values of K than the range shown. Parameters: $\sigma = 0.1, \Omega_0 = 1$.

C. Transmission delay

We now consider transmission delays, as in [30, 55, 63], modelling a signal which travels between oscillators at a constant velocity. We have

$$\frac{d\theta_j(t)}{dt} = \omega_j + \frac{K}{2M+1}\sum_{k=-M}^{M}\sin\left[\theta_{j+k}(t-|k|\Delta x s) - \theta_j(t)\right] \tag{25}$$

where $\Delta x = 2\pi/N$ and s is the reciprocal of the transmission velocity, i.e. the delay is proportional to the distance between oscillators. We define the complex mean field at each point by

$$Z_j(t) = \frac{1}{2M+1}\sum_{k=-M}^{M} e^{i\theta_{j+k}(t-|k|\Delta x s)} \tag{26}$$

Moving to the continuum limit and performing the integrals as in Sec. II A we obtain

$$\frac{\partial u}{\partial t} = (-1+i\Omega_0)u + \frac{K}{2}\left[Z - \overline{Z}u^2\right] \tag{27}$$

as in Sec. II A, but where

$$Z(x,t) = \int_0^{2\pi} G(x-y)u(y, t-|x-y|s)dy \tag{28}$$

and $|x-y|$ denotes the shortest distance between points x and y on the circle, i.e. $|x-y| = \min(|x-y|, 2\pi - |x-y|)$. For a twisted state $u(x,t) = ae^{i(qx+\nu t)}$ and coupling function (6)

$$Z(x,t) = \frac{iae^{i(qx+\nu t)}}{4\pi\sigma}\left[\frac{1-e^{2\pi i\sigma(q-\nu s)}}{q-\nu s} - \frac{1-e^{-2\pi i\sigma(q+\nu s)}}{q+\nu s}\right] \tag{29}$$

and thus twisted states are solutions of

$$i\nu = -1 + i\Omega_0 + \frac{K}{2}\left[\eta - \bar{\eta}a^2\right] \tag{30}$$

where

$$\eta \equiv \frac{i}{4\pi\sigma}\left[\frac{1-e^{2\pi i\sigma(q-\nu s)}}{q-\nu s} - \frac{1-e^{-2\pi i\sigma(q+\nu s)}}{q+\nu s}\right] \tag{31}$$

Setting $a = 0$ we find that for fixed σ and s a q-twisted state is created at

$$K = \frac{2}{\mathrm{Re}(\eta)} \tag{32}$$

where ν is a solution of

$$\nu = \Omega_0 + \frac{\mathrm{Im}(\eta)}{\mathrm{Re}(\eta)} \tag{33}$$

We know that for $s = 0$, $\mathrm{Im}(\eta) = 0$ and thus $\nu = \Omega_0$ and a q-twisted state is created at $K = 2/\widehat{G}(q)$. Following these bifurcations as s is increased from zero we obtain the curves shown with solid lines in Fig. 4. The stability of these solutions was found by direct simulation to change via a Hopf bifurcation at the points indicated by circles in Fig. 4. We see that for these parameter values, increasing s, i.e. decreasing the transmission velocity, moves all curves to higher values of K.

We finish this section by noting that when performing the reduction of general weakly coupled oscillators with transmission delay to phase oscillators, the delay appears as a phase shift, i.e. one obtains an undelayed system of the form

$$\frac{d\theta_j}{dt} = \omega_j + \frac{K}{2M+1}\sum_{k=-M}^{M}\sin\left(\theta_{j+k} - \theta_j - \alpha|k|\Delta x\right) \tag{34}$$

where α is a constant [7, 15]. We will not consider such a system here.

D. Distributed delay

We now consider distributed delays. Let us define the complex mean field as in (3) but then suppose that oscillator j is influenced by a delayed version of Z_j, as in [31, 39], i.e. define

$$R_j(t) = \int_0^\infty Z_j(t-\Delta)h(\Delta)d\Delta \tag{35}$$

where $h(\Delta)$ is the probability density of the delay Δ, and let the oscillator dynamics be

$$\frac{d\theta_j}{dt} = \omega_j + K\mathrm{Im}\left[R_j e^{-i\theta_j}\right] = \omega_j + \frac{K}{2i}\left[R_j e^{-i\theta_j} - \overline{R}_j e^{i\theta_j}\right] \tag{36}$$

(As presented, we calculate $R_j(t)$ by first forming the local mean field and then delaying it. Since the sum in (3) and the integral in (35) commute we can also think of $R_j(t)$ as resulting from first delaying all the θs and then forming the local mean field from those delayed values.) Moving to the continuum limit and performing the integrals as above we obtain

$$\frac{\partial u(x,t)}{\partial t} = (-1+i\Omega_0)u(x,t) + \frac{K}{2}\left[R(x,t) - \overline{R}(x,t)u^2(x,t)\right] \tag{37}$$

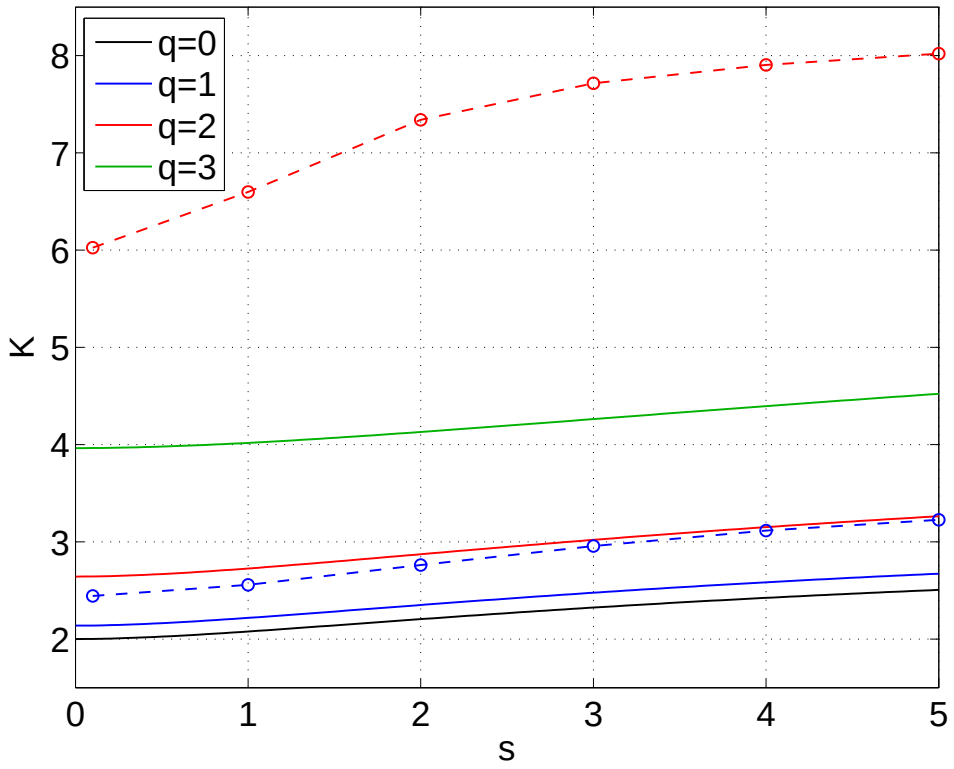

FIG. 4: q-twisted states for the case of transmission delays are created as the corresponding solid line is crossed from below, and become stable as the dashed line of the same colour is crossed from below. The $q = 0$ state is stable upon creation and the $q = 3$ state is stabilised at higher values of K than the range shown. Parameters: $\sigma = 0.1, \Omega_0 = 1$.

where

$$R(x,t) = \int_0^\infty Z(x, t-\Delta)h(\Delta)d\Delta \tag{38}$$

If $h(\Delta) = \delta(\Delta - \tau)$ we have $R(x,t) = Z(x, t-\tau)$ and we recover the model in Sec. II B. Alternatively, suppose that $h(\Delta) = \tau^{-1}e^{-\Delta/\tau}$, a choice which allows analytical progress. Using the linear chain trick one can write (38) as

$$\tau\frac{\partial R(x,t)}{\partial t} = Z(x,t) - R(x,t) \tag{39}$$

(Distributions of the form $h(\Delta) \sim \Delta^n e^{-\Delta/\tau}$ for positive integer n also allow (38) to be written as a differential equation for R [38, 39].) For a twisted state $u(x,t) = ae^{i(qx+\nu t)}$, (37) and (39) give

$$i\nu = -1 + i\Omega_0 + \frac{K\widehat{G}(q)}{2}\left(\frac{1}{1+i\nu\tau} - \frac{a^2}{1-i\nu\tau}\right) \tag{40}$$

Rearranging we find that

$$a^2 = 1 - \frac{2(1+\nu^2\tau^2)}{K\widehat{G}(q)} \tag{41}$$

where ν satisfies

$$\nu = \Omega_0 + \frac{\nu\tau\left[1+\nu^2\tau^2 - K\widehat{G}(q)\right]}{1+\nu^2\tau^2} \tag{42}$$

Setting $a = 0$ we find that a q-twisted state is created at

$$K = \frac{2}{\widehat{G}(q)}\left(1 + \frac{\tau^2\Omega_0^2}{(1+\tau)^2}\right) \tag{43}$$

Instead of varying τ we will set $\tau = 2$ and vary Ω_0, as doing so leads to some interesting behaviour [31, 39]. As in Sec. II B we move to a rotating coordinate frame at speed ν, i.e. let $\tilde{u}(x,t) = u(x,t)e^{-i\nu t}, \widetilde{R}(x,t) = R(x,t)e^{-i\nu t}$ and $\widetilde{Z}(x,t) = Z(x,t)e^{-i\nu t}$ so that $\tilde{u}$ is a fixed point of

$$\frac{\partial\tilde{u}(x,t)}{\partial t} = (-1 + i(\Omega_0 - \nu))\tilde{u}(x,t) + \frac{K}{2}\left[\widetilde{R}(x,t) - \overline{\widetilde{R}}(x,t)\tilde{u}^2(x,t)\right] \tag{44}$$

where

$$\tau\frac{\partial\widetilde{R}(x,t)}{\partial t} = \widetilde{Z}(x,t) - \widetilde{R}(x,t) - i\nu\tau\widetilde{R}(x,t) \tag{45}$$

and

$$\widetilde{Z}(x,t) = \int_0^{2\pi} G(x-y)\tilde{u}(y,t)dy \tag{46}$$

Following bifurcations of twisted states we obtain the results in Fig. 5. For Ω_0 small we obtain similar results to previous sections, but for larger Ω_0 we see that twisted states are created in saddle-node bifurcations as K is increased. In this range the bifurcation from the zero state is subcritical, leading to the creation of an unstable branch which is stabilised through either a saddle-node bifurcation (for $q = 0$) or in a Hopf bifurcation (for $q > 0$).

Figure 6 shows a plot of a versus K for $\Omega_0 = 2.5$, i.e. at the right edge of Fig. 5. Recalling that the zero state is stable for $K < 2[1 + (\tau\Omega_0/(1+\tau))^2]$ (68/9 for the parameters used here) we see the possibility of bistability between the zero state and twisted states with low twist. Thus we could initialise part of the domain at the zero state and the remainder at a twisted state and follow the system's evolution. This is shown in Fig. 7 for three different initial conditions. (We have spatially discretised (37) and (39) using $N = 500$ points, with a neighbourhood of $M = 5$. Boundary conditions are not periodic. To evaluate the sums near the boundaries, we extrapolate both the amplitude and phase of u to a further M points outside of the domain shown. For a periodic domain of length 2π, q must be an integer. For non-periodic boundary conditions q can be any real number, and is then a measure of the *twist rate*, i.e. the spatial rate at which θ varies. Thus Fig. 6 cannot be used to perfectly *predict* the behaviour in Fig. 7, but to *suggest* what might occur.)

In Fig. 7 we see that the "front" joining the twisted and the zero state travels at a uniform speed, which depends on the twist rate of the twisted part of the pattern. Such patterns would be stationary in the appropriate simultaneously travelling and rotating coordinate frame and could be studied using the techniques in [31]. It is also possible to obtain stable spatially-localised "bumps" of synchronous activity in a background of asynchrony ($u = 0$) by choosing appropriate parameter values and initial conditions, as in Fig. 8.

We now move to considering travelling waves in a network of coupled theta neurons, each of which is also described by a single angular variable.

III. THETA NEURONS

The theta neuron is a canonical model for a neuron which undergoes a saddle-node-on-invariant-circle bifurcation as its input current is increased [12, 13, 19]. It can be derived from the quadratic integrate-and-fire neuron [37] via a coordinate transformation. The state of a neuron is described by a single angular variable, θ, and the neuron is said to "fire" when θ increases through π.

A. Theory

Suppose we have a network of N heterogeneous theta neurons equally spaced on a domain of length 1 with periodic boundary conditions, coupled via instantaneous synapses to themselves and

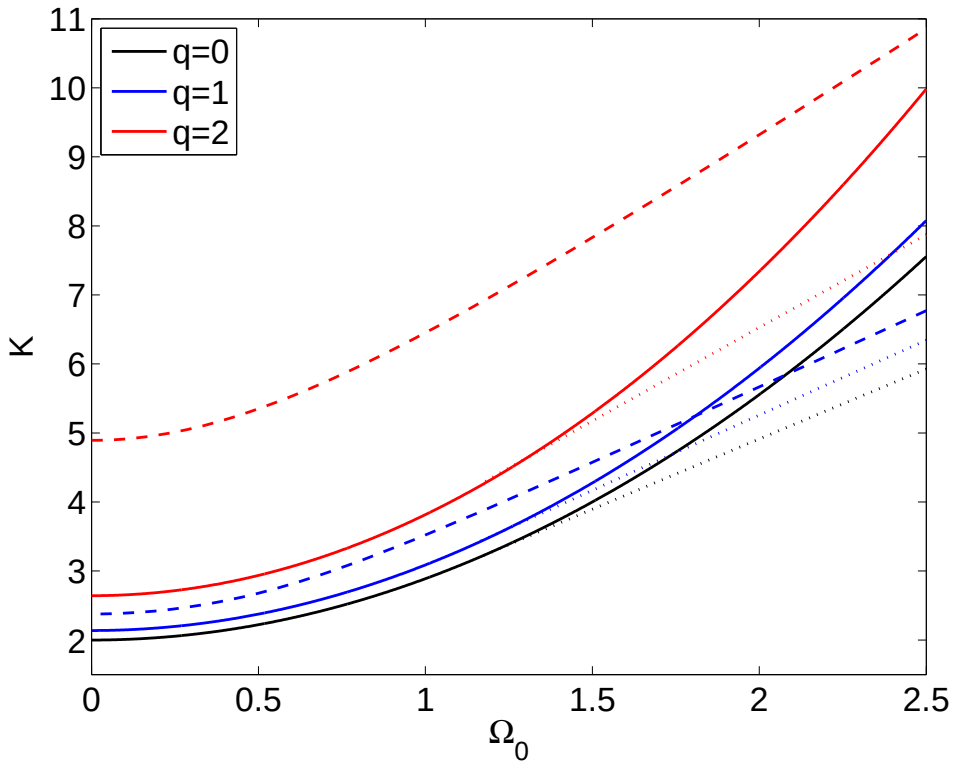

FIG. 5: q-twisted states for the case of distributed delays bifurcate from the zero state as the corresponding solid line is crossed, and become stable as the dashed line of the same colour is crossed from below. The $q = 0$ state is stable upon creation as K is increased. For larger Ω_0, the states are created in saddle-node bifurcations (dotted). Parameters: $\sigma = 0.1, \tau = 2$.

their nearest M neighbours to the right equally with strength g. Such asymmetric coupling has been studied in a neural context in [6, 61] for example, as a mechanism for generating travelling waves. See also [9, 20, 26, 27, 35] for chains of coupled oscillators with asymmetric coupling. The model neurons are governed by

$$\frac{d\theta_j}{dt} = 1 - \cos\theta_j + (1 + \cos\theta_j)(I_j + g s_j); \qquad j = 1, 2, \ldots N \tag{47}$$

where

$$s_j = \frac{a_n}{N} \sum_{k=0}^{M} (1 - \cos\theta_{j+k})^n \tag{48}$$

indices are taken mod N, and a_n is the normalisation factor $a_n = 2^n (n!)^2/(2n)!$. The function $(1 - \cos\theta)^n$ is meant to mimic the action potential produced when a neuron fires. I_j is the input current to neuron j in the absence of any coupling and since neurons are not expected to be identical, it is natural to assume that this quantity is different for each neuron. Thus the I_j are assumed to be randomly chosen from a Lorentzian with mean I_0 and half-width-at-half-maximum Δ, as others have done [32, 34, 40, 42, 56] (although see [29]). Note that unlike the model considered in Sec. II, (47) is not invariant under a uniform phase shift applied to all neurons. We take the continuum limit $M, N \to \infty$ in such a way that $M/N \to \lambda < 1$ and describe the network by a probability density function, as in Sec. II A. Following similar analysis as in that section (or see [32, 34, 40, 56]) we obtain

$$\frac{\partial z}{\partial t} = \frac{(iI_0 - \Delta)(1 + z)^2 - i(1 - z)^2}{2} + \frac{ig(1 + z)^2 S}{2} \tag{49}$$

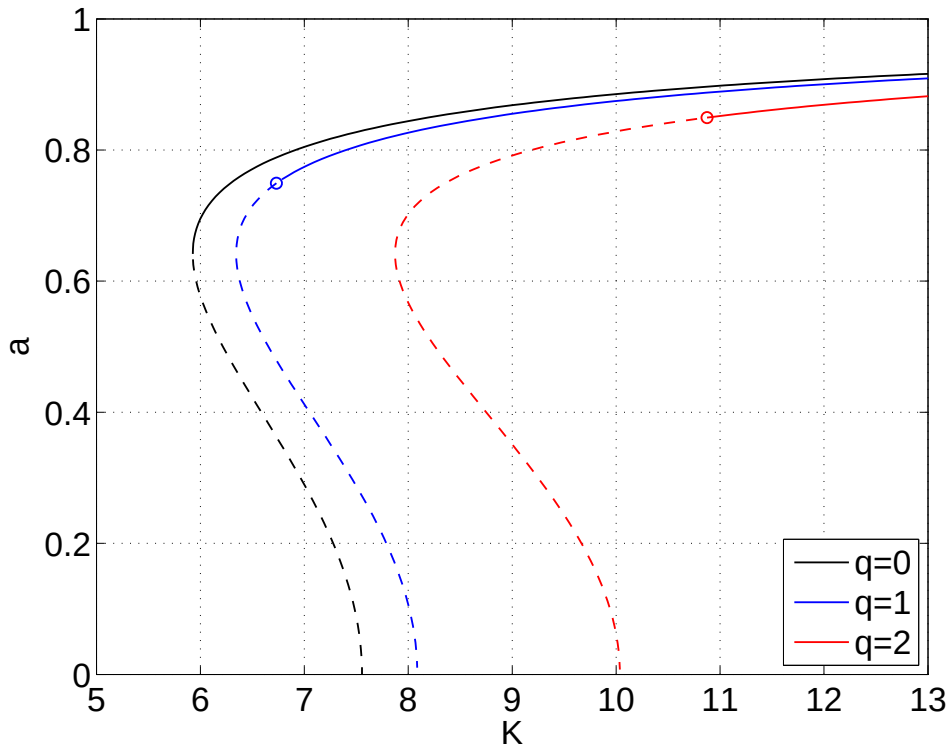

FIG. 6: a as a function of K for twisted states with $q = 0, 1$ and 2. Solid: stable; dashed: unstable. Hopf bifurcations are indicated by the circles. Parameters: $\sigma = 0.1, \tau = 2, \Omega_0 = 2.5$.

where

$$S(x,t) = \int_0^\lambda H(z(x+y,t);n)\ dy \tag{50}$$

and the integral is evaluated using periodic boundary conditions, and

$$H(z;n) = a_n \left[C_0 + \sum_{j=1}^{n} C_j (z^j + \bar{z}^j) \right] \tag{51}$$

where

$$C_j = \sum_{k=0}^{n} \sum_{m=0}^{k} \frac{n!(-1)^k \delta_{k-2m,j}}{2^k (n-k)! m! (k-m)!}\ . \tag{52}$$

$z(x,t)$ is the usual Kuramoto order parameter at position x and time t, i.e. the expected value of $e^{i\theta}$ [57]. The instantaneous firing frequency of the network at position x and time t is given by [34, 42]

$$f(x,t) = \frac{1}{\pi} \mathrm{Re} \left(\frac{1 - \bar{z}(x,t)}{1 + \bar{z}(x,t)} \right) \tag{53}$$

B. No delay

First consider the case of no delays. A simulation of the network of neurons (47)-(48) shows a stable travelling pulse (Fig. 9). The corresponding pulse in the continuum equations (49)-(50) is

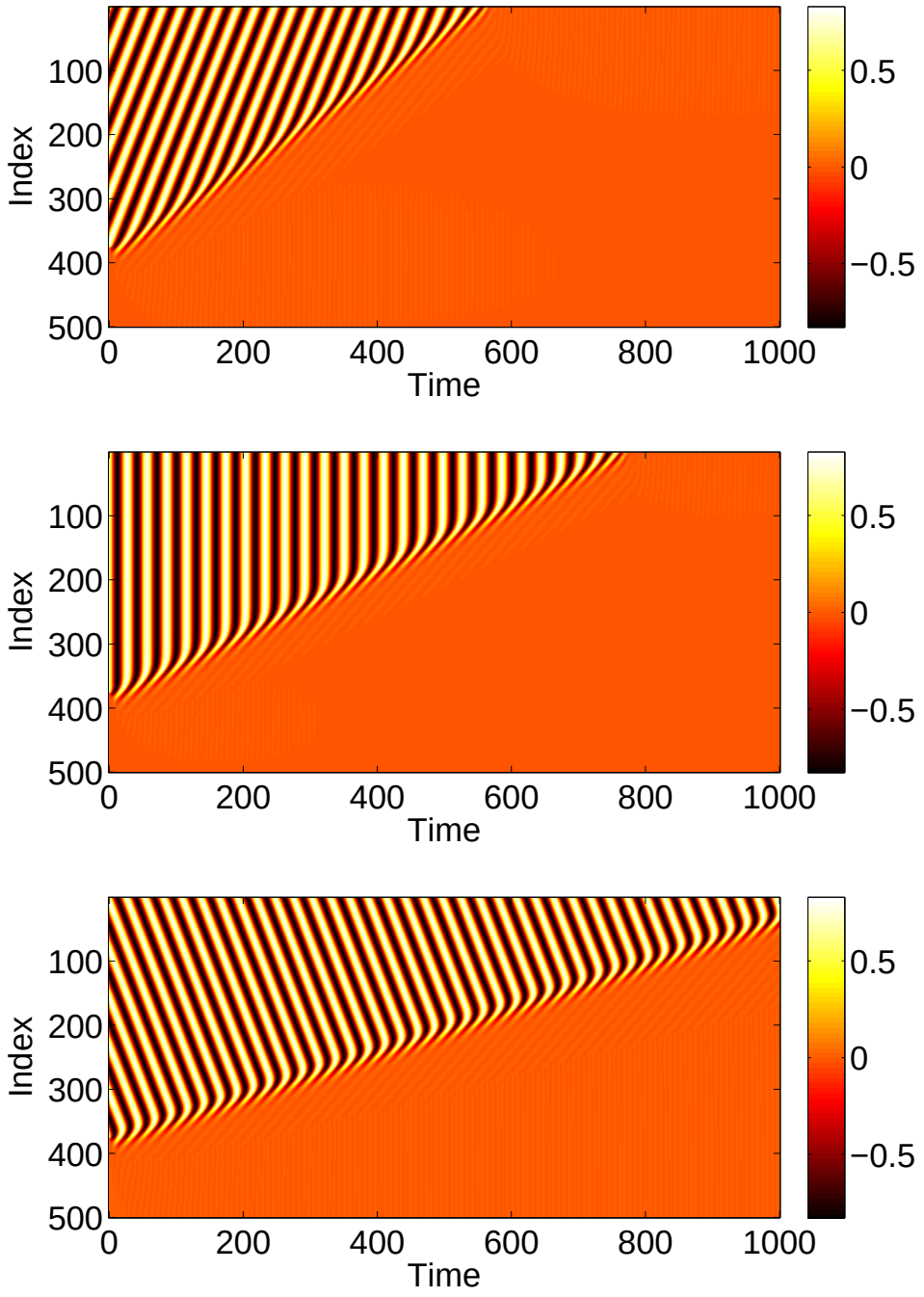

FIG. 7: Solutions of (37)-(38). Re(u) is shown color-coded for three different initial conditions. For the upper and lower panels, the twisted parts of the initial conditions have twists of opposite signs, whereas for the middle panel it has zero twist. The front joining the twisted state to the zero state has highest speed in the upper panel and lowest in the lower. Note that boundary conditions are not periodic. Parameters: $N = 500, M = 5, K = 7.5, \tau = 2, \Omega_0 = 2.5$.

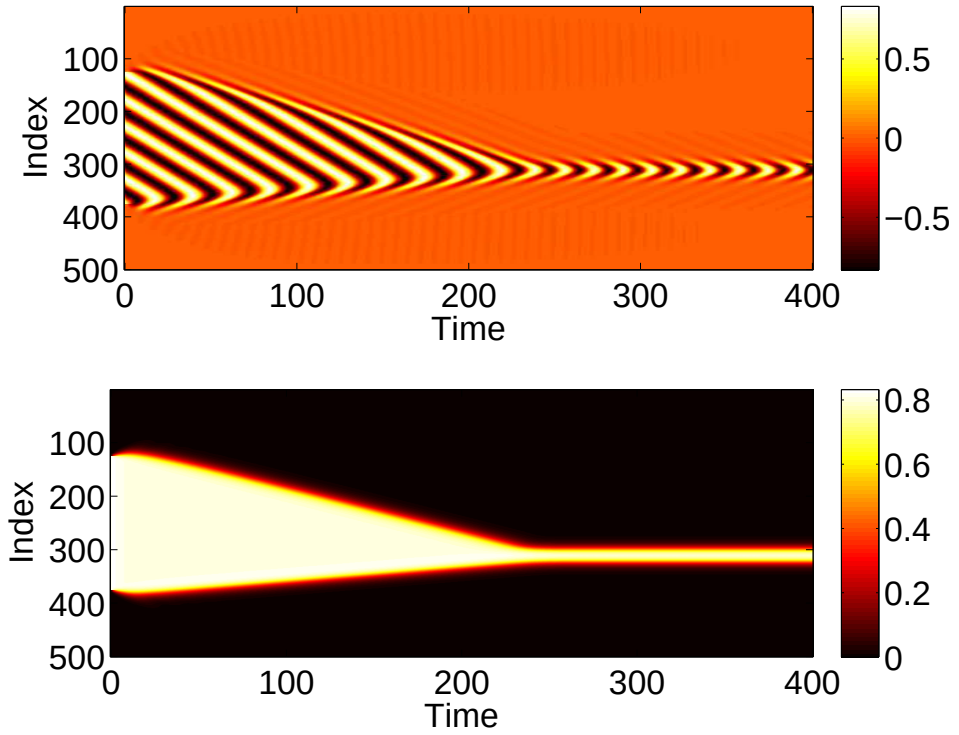

FIG. 8: Solutions of (37)-(38). Top: Re(u); bottom: $|u|$, shown color-coded. Parameters as in Fig. 7.

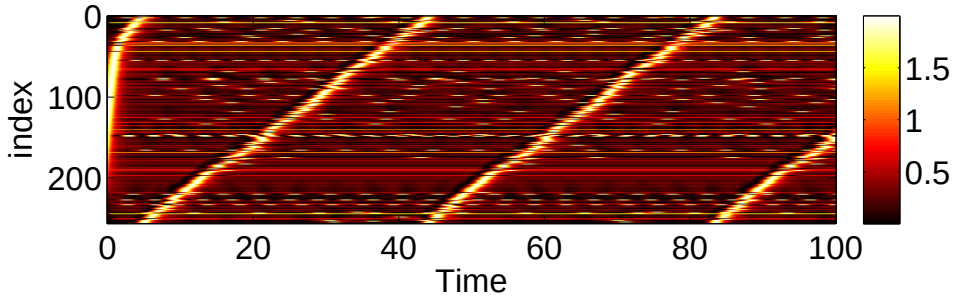

FIG. 9: Travelling wave solution of (47)-(48). $1-\cos\theta$ is shown in colour. Parameters: $N=256, M=16, I_0=-0.2, \Delta=0.05, g=11, n=2$.

shown in Fig. 10. These pulses move with a fixed profile at a constant speed. Note that the argument of z increases through π once as we move around the domain, and this point corresponds to the maximum of the firing frequency, as expected. (The network also supports travelling pulses with more than one active region, but we do not consider them here.) Travelling waves such as that in Fig. 9 have been observed in a number of neural systems [5, 51].

An important difference between the solution in Fig. 10 and the uniformly twisted states studied in Sec. II is that the twisted states can be characterised completely by the amplitude of z and the twist rate, whereas to describe a solution like that in Fig. 10 we need the actual shape of the pulse, i.e. $z(x,t)$ at some given time t. Thus the existence and stability of these solutions, as well as their speed, must be determined numerically. Letting $\xi = x + ct$, (49)-(50) become

$$\frac{\partial z(\xi,t)}{\partial t} = -c\frac{\partial z(\xi,t)}{\partial \xi} + \frac{(iI_0-\Delta)(1+z(\xi,t))^2 - i(1-z(\xi,t))^2}{2} + \frac{ig(1+z(\xi,t))^2 S(\xi,t)}{2} \qquad (54)$$

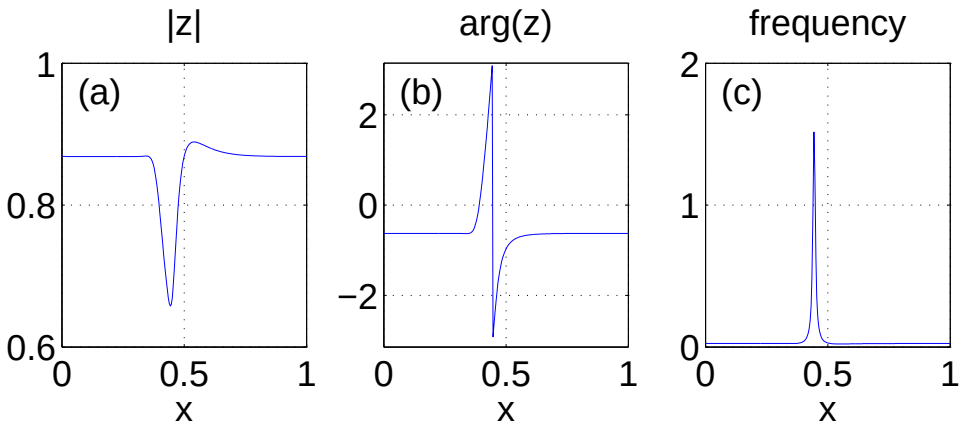

FIG. 10: Travelling wave solution of (49)-(50) (moving to the left at constant speed). (a): $|z|$; (b): $\arg(z)$; (c): instantaneous frequency. Parameters: $I_0 = -0.2, \Delta = 0.05, g = 11, n = 2, \lambda = 1/16$.

where

$$S(\xi, t) = \int_0^\lambda H(z(\xi + y, t); n)\ dy \tag{55}$$

If c (taken to be positive) is the speed of a wave like that in Fig. 10, the wave will be stationary in the (ξ, t) coordinate system, i.e. it will satisfy

$$0 = -c\frac{dz(\xi)}{d\xi} + \frac{(iI_0 - \Delta)(1 + z(\xi))^2 - i(1 - z(\xi))^2}{2} + \frac{ig(1 + z(\xi))^2 S(\xi)}{2} \tag{56}$$

where

$$S(\xi) = \int_0^\lambda H(z(\xi + y); n)\ dy \tag{57}$$

We can numerically follow solutions of (56)-(57) as parameters are varied and determine their stability by linearising (54) about them [33]. Varying g, for example, we obtain Fig. 11. As g is decreased the wave is destroyed in a saddle-node bifurcation, and as g is increased it becomes unstable through a Hopf bifurcation.

C. Distributed delay

We now consider a distributed delay, as in Sec. II D. The oscillator equations are still (47), but we have

$$s_j(t) = \frac{a_n}{N}\int_0^\infty h(\Delta)\sum_{k=0}^{M}[1 - \cos\theta_{j+k}(t - \Delta)]^n\ d\Delta \tag{58}$$

where $h(\Delta)$ is the distribution of delays. Choosing $h(\Delta) = \tau^{-1}e^{-\Delta/\tau}$ we have

$$\tau\frac{ds_j}{dt} = \frac{a_n}{N}\sum_{k=0}^{M}(1 - \cos\theta_{j+k})^n - s_j \tag{59}$$

where all variables are evaluated at the same time. (This type of synaptic dynamics is commonly used [4, 14].) Taking the continuum limit we obtain (49) but with

$$\tau\frac{\partial S(x,t)}{\partial t} = \int_0^\lambda H(z(x + y, t); n)\ dy - S(x, t) \tag{60}$$

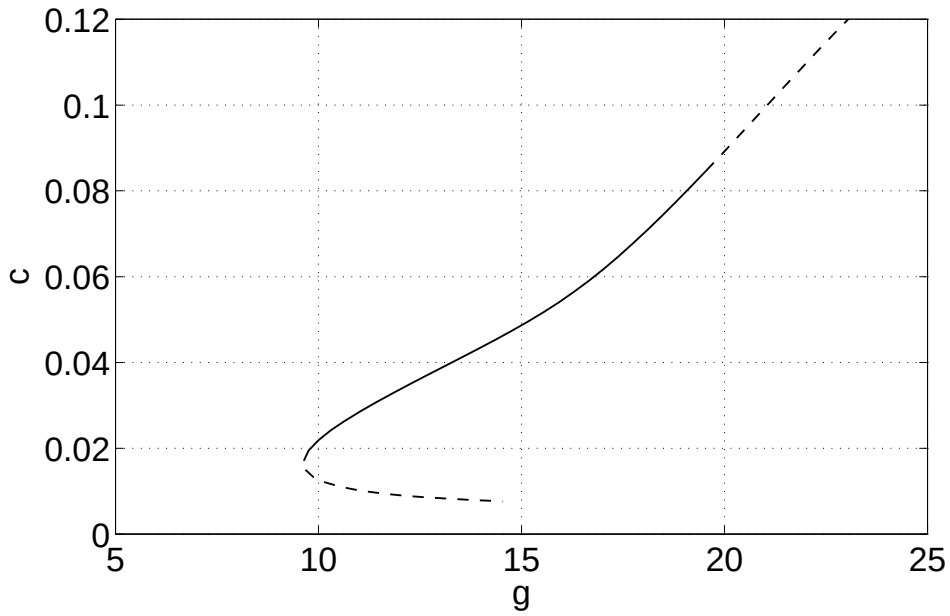

FIG. 11: Speed of travelling wave solution of (49)-(50) as a function of g. Solid: stable; dashed: unstable. Parameters: $I_0 = -0.2, \Delta = 0.05, n = 2, \lambda = 1/16$.

Setting $\tau = 0$ we obtain a model of the form studied in [32, 34]. Varying both g and τ we obtain the results in Fig. 12. Increasing τ decreases the range of values of g over which the travelling wave exists. For large enough τ the travelling wave is destroyed in saddle-node bifurcations for g both too small and too large.

IV. SUMMARY AND DISCUSSION

We have investigated the effects of including several forms of delays on the dynamics of uniformly twisted waves in networks of non-locally coupled Kuramoto oscillators, and of travelling waves in similar networks of model theta neurons. Our work can be regarded as a generalisations of the results in [45] and [32]. For both types of networks the state of an oscillator is described by a single angular variable, and the Ott/Antonsen (OA) ansatz can be used to derive exact equations governing the asymptotic (in time) evolution of an order parameter in the continuum limit. The existence of uniformly twisted waves can be determined analytically, due to their simple form, but travelling waves in networks of theta neurons must be found numerically.

For the parameters used, we found that increasing both constant and transmission delays moved the existence and stability of uniformly twisted waves in Kuramoto networks to higher values of the coupling strength (Figs. 3 and 4). A distributed delay allowed bistability between the zero state and a uniformly twisted state and thus the possibility of fronts joining these two states (Fig. 7). For the network of theta neurons, increasing the value of the distributed delay time constant led to eventual destruction of the travelling wave (Fig. 12). Even the simple networks considered here have a number of parameters which must be set, and the results found here will differ for different values of these parameters.

The OA ansatz restricts the probability density for the phases to a particular manifold, parametrised by a complex, spatially-dependent variable. For the systems studied here this manifold is invariant, and the dynamics on it are given by equations of the form (12)-(13). However, the global attractiveness of this manifold has only been determined in some cases and not (as far as we are aware) for a system like (47), where, in the continuum limit, the coefficient of a sinusoidal fuction of θ is distributed. Nonetheless, using the ansatz for networks of theta neurons does seem to correctly predict the behaviour of large networks [32, 34, 40]. Also note that since the OA ansatz restricts the probability density to a particular manifold, it will not capture transients of the original network

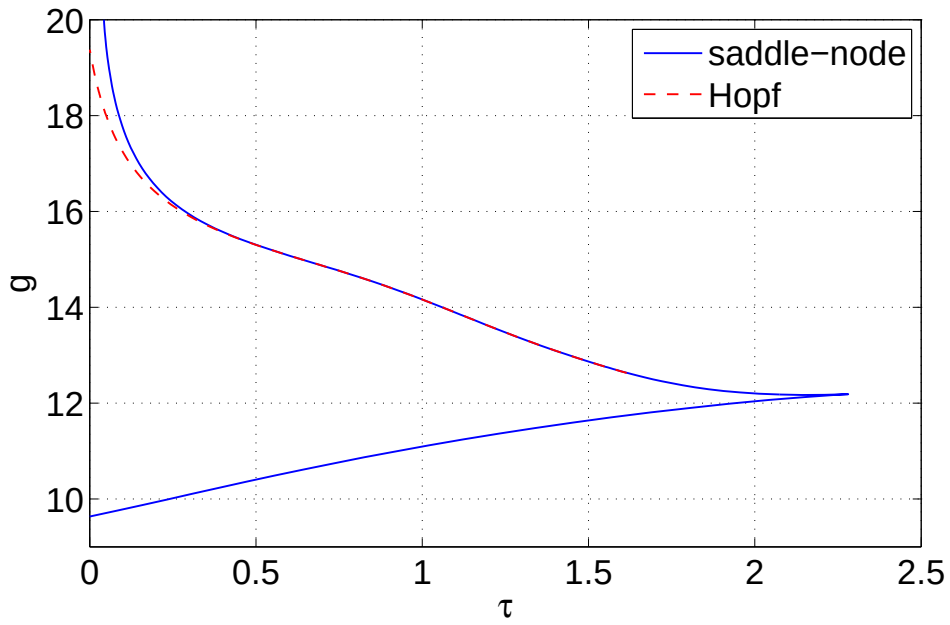

FIG. 12: Curves of saddle-node (solid) and Hopf (dashed) bifurcations of travelling wave solution of (49),(60). The curves meet at a Takens-Bogdanov bifurcation. A travelling wave solution like that in Fig. 10 exists in the region between the two solid blue curves. $\tau = 0$ corresponds to Fig. 11. Parameters: $I_0 = -0.2, \Delta = 0.05, n = 2, \lambda = 1/16$.

which are not on this manifold.

Regarding generalisations, we have considered only phase oscillators, and it would be of interest to determine which of our results qualitatively agree with those for networks of more general oscillators. We have considered only the case of non-identical oscillators, as it is then that the OA ansatz is thought to be valid. However, it would also be of interest to consider the case of identical oscillators as in [59], and then including delays, as in, for example [53–55]. Other possible generalisations include considering two-dimensional domains [22, 25], and forms of heterogeneity other than Lorentzian [29].

Acknowledgements: I thank the referees for their helpful comments.

[1] J.A. Acebrón, LL Bonilla, C.J. Pérez Vicente, F. Ritort, and R. Spigler. The Kuramoto model: A simple paradigm for synchronization phenomena. *Rev. Mod. Phys.*, 77(1):137–185, 2005.

[2] Samuel Bernard, Jacques Bélair, and Michael C Mackey. Sufficient conditions for stability of linear differential equations with distributed delay. *Discrete and Continuous Dynamical Systems Series B*, 1(2):233–256, 2001.

[3] Ingo Bojak and David TJ Liley. Axonal velocity distributions in neural field equations. *PLoS Comput Biol*, 6(1):e1000653, 2010.

[4] Christoph Börgers and Nancy Kopell. Synchronization in networks of excitatory and inhibitory neurons with sparse, random connectivity. *Neural computation*, 15(3):509–538, 2003.

[5] Paul C Bressloff. Waves in neural media. *Lecture Notes on Mathematical Modelling in the Life Sciences, Springer, New York*, 2014.

[6] Paul C Bressloff and Jeremy Wilkerson. Traveling pulses in a stochastic neural field model of direction selectivity. *Frontiers in computational neuroscience*, 6, 2012.

[7] S.M. Crook, G.B. Ermentrout, M.C. Vanier, and J.M. Bower. The role of axonal delay in the synchronization of networks of coupled cortical oscillators. *Journal of computational neuroscience*, 4(2):161–172, 1997.

[8] Alain Destexhe, Zachary F Mainen, and Terrence J Sejnowski. Synthesis of models for excitable membranes, synaptic transmission and neuromodulation using a common kinetic formalism. *Journal of computational neuroscience*, 1(3):195–230, 1994.

[9] O. D'Huys, R. Vicente, T. Erneux, J. Danckaert, and I. Fischer. Synchronization properties of network motifs: Influence of coupling delay and symmetry. *Chaos*, 18(3), 2008.

[10] Matthew G. Earl and Steven H. Strogatz. Synchronization in oscillator networks with delayed coupling: A stability criterion. *Phys. Rev. E*, 67:036204, Mar 2003.

[11] Koen Engelborghs, Tatyana Luzyanina, and Dirk Roose. Numerical bifurcation analysis of delay differential equations using dde-biftool. *ACM Transactions on Mathematical Software (TOMS)*, 28(1):1–21, 2002.

[12] B. Ermentrout. Ermentrout-Kopell canonical model. *Scholarpedia*, 3(3):1398, 2008.

[13] Bard Ermentrout. Type i membranes, phase resetting curves, and synchrony. *Neural computation*, 8(5):979–1001, 1996.

[14] Bard Ermentrout. Gap junctions destroy persistent states in excitatory networks. *Physical Review E*, 74(3):031918, 2006.

[15] Bard Ermentrout and Tae-Wook Ko. Delays and weakly coupled neuronal oscillators. *Philosophical Transactions of the Royal Society of London A: Mathematical, Physical and Engineering Sciences*, 367(1891):1097–1115, 2009.

[16] G.B. Ermentrout and D. Terman. *Mathematical Foundations of Neuroscience*, volume 35. Springer Verlag, 2010.

[17] T. Girnyk, M. Hasler, and Y. Maistrenko. Multistability of twisted states in non-locally coupled kuramoto-type models. *Chaos: An Interdisciplinary Journal of Nonlinear Science*, 22(1):013114–013114, 2012.

[18] David Golomb and G Bard Ermentrout. Effects of delay on the type and velocity of travelling pulses in neuronal networks with spatially decaying connectivity. *Network: Computation in Neural Systems*, 11(3):221–246, 2000.

[19] Boris Gutkin. Theta-neuron model. In Dieter Jaeger and Ranu Jung, editors, *Encyclopedia of Computational Neuroscience*, pages 1–9. Springer New York, 2014.

[20] Seung-Yeal Ha and Moon-Jin Kang. On the basin of attractors for the unidirectionally coupled kuramoto model in a ring. *SIAM Journal on Applied Mathematics*, 72(5):1549–1574, 2012.

[21] Stewart Heitmann and G Bard Ermentrout. Synchrony, waves and ripple in spatially coupled kuramoto oscillators with mexican hat connectivity. *Biological cybernetics*, pages 1–15, 2015.

[22] Seong-Ok Jeong, Tae-Wook Ko, and Hie-Tae Moon. Time-delayed spatial patterns in a two-dimensional array of coupled oscillators. *Phys. Rev. Lett.*, 89:154104, Sep 2002.

[23] Uhnoh Kim, Thierry Bal, and David A McCormick. Spindle waves are propagating synchronized oscillations in the ferret LGNd in vitro. *Journal of Neurophysiology*, 74(3):1301–1323, 1995.

[24] Tae-Wook Ko and G Bard Ermentrout. Effects of axonal time delay on synchronization and wave formation in sparsely coupled neuronal oscillators. *Physical Review E*, 76(5):056206, 2007.

[25] Tae-Wook Ko, Seong-Ok Jeong, and Hie-Tae Moon. Wave formation by time delays in randomly coupled oscillators. *Physical Review E*, 69(5):056106, 2004.

[26] N. Kopell, W. Zhang, and G. B. Ermentrout. Multiple coupling in chains of oscillators. *SIAM Journal on Mathematical Analysis*, 21(4):935–953, 1990.

[27] Nancy Kopell and GB Ermentrout. Symmetry and phaselocking in chains of weakly coupled oscillators. *Communications on Pure and Applied Mathematics*, 39(5):623–660, 1986.

[28] Y. Kuramoto. *Chemical Oscillations, Waves, and Turbulence*. Springer, Berlin, 1984.

[29] Luis F Lafuerza, Pere Colet, and Raul Toral. Nonuniversal results induced by diversity distribution in coupled excitable systems. *Physical review letters*, 105(8):084101, 2010.

[30] Carlo R. Laing. The dynamics of chimera states in heterogeneous kuramoto networks. *Physica D*, 238(16):1569–1588, 2009.

[31] Carlo R. Laing. Fronts and bumps in spatially extended kuramoto networks. *Physica D: Nonlinear Phenomena*, 240(24):1960 – 1971, 2011.

[32] Carlo R Laing. Derivation of a neural field model from a network of theta neurons. *Physical Review E*, 90(1):010901, 2014.

[33] Carlo R. Laing. Numerical bifurcation theory for high-dimensional neural models. *Journal of Mathematical Neuroscience*, 4(1):13, 2014.

[34] Carlo R. Laing. Exact neural fields incorporating gap junctions. *SIAM Journal on Applied Dynamical Systems*, 14(4):1899–1929, 2015.

[35] OE Lanford III and SM Mintchev. Stability of a family of travelling wave solutions in a feedforward chain of phase oscillators. *Nonlinearity*, 28(1):237, 2015.

[36] R. Lang and K. Kobayashi. External optical feedback effects on semiconductor injection laser properties. *IEEE Journal of Quantum Electronics*, 16(3):347–355, 1980.

[37] PE Latham, BJ Richmond, PG Nelson, and S Nirenberg. Intrinsic dynamics in neuronal networks. i. theory. *Journal of Neurophysiology*, 83(2):808–827, 2000.

[38] Wai Shing Lee, Edward Ott, and Thomas M. Antonsen. Large coupled oscillator systems with heterogeneous interaction delays. *Phys. Rev. Lett.*, 103:044101, Jul 2009.

[39] Wai Shing Lee, Juan G. Restrepo, Edward Ott, and Thomas M. Antonsen. Dynamics and pattern formation in large systems of spatially-coupled oscillators with finite response times. *Chaos*, 21(2):023122,

2011.

[40] Tanushree B Luke, Ernest Barreto, and Paul So. Complete classification of the macroscopic behavior of a heterogeneous network of theta neurons. *Neural computation*, 25(12):3207–3234, 2013.

[41] Georgi S Medvedev. Small-world networks of kuramoto oscillators. *Physica D: Nonlinear Phenomena*, 266:13–22, 2014.

[42] Ernest Montbrió, Diego Pazó, and Alex Roxin. Macroscopic description for networks of spiking neurons. *Phys. Rev. X*, 5:021028, Jun 2015.

[43] Ernest Montbrió, Diego Pazó, and Jürgen Schmidt. Time delay in the kuramoto model with bimodal frequency distribution. *Physical Review E*, 74(5):056201, 2006.

[44] O E Omel'chenko. Coherence-incoherence patterns in a ring of non-locally coupled phase oscillators. *Nonlinearity*, 26(9):2469, 2013.

[45] Oleh E Omel'chenko, Matthias Wolfrum, and Carlo R Laing. Partially coherent twisted states in arrays of coupled phase oscillators. *Chaos: An Interdisciplinary Journal of Nonlinear Science*, 24(2):023102, 2014.

[46] Edward Ott and Thomas M. Antonsen. Low dimensional behavior of large systems of globally coupled oscillators. *Chaos*, 18(3):037113, 2008.

[47] Edward Ott and Thomas M. Antonsen. Long time evolution of phase oscillator systems. *Chaos*, 19(2):023117, 2009.

[48] Mark J Panaggio and Daniel M Abrams. Chimera states: coexistence of coherence and incoherence in networks of coupled oscillators. *Nonlinearity*, 28(3):R67, 2015.

[49] A. Pikovsky, M. Rosenblum, and J. Kurths. *Synchronization*. Cambridge U. Press, Cambridge, U. K., 2003.

[50] David J Pinto and G Bard Ermentrout. Spatially structured activity in synaptically coupled neuronal networks: I. traveling fronts and pulses. *SIAM journal on Applied Mathematics*, 62(1):206–225, 2001.

[51] David J Pinto, Saundra L Patrick, Wendy C Huang, and Barry W Connors. Initiation, propagation, and termination of epileptiform activity in rodent neocortex in vitro involve distinct mechanisms. *The Journal of neuroscience*, 25(36):8131–8140, 2005.

[52] Francisco A. Rodrigues, Thomas K. DM. Peron, Peng Ji, and Jürgen Kurths. The kuramoto model in complex networks. *Physics Reports*, pages –, 2015.

[53] Gautam C Sethia, Abhijit Sen, and Fatihcan M Atay. Phase-locked solutions and their stability in the presence of propagation delays. *Pramana*, 77(5):905–915, 2011.

[54] G.C. Sethia, A. Sen, and F.M. Atay. Clustered chimera states in delay-coupled oscillator systems. *Phys. Rev. Lett.*, 100(14):144102, 2008.

[55] G.C. Sethia, A. Sen, and F.M. Atay. Synchronous solutions and their stability in nonlocally coupled phase oscillators with propagation delays. *Physical Review E*, 81(5):056213, 2010.

[56] Paul So, Tanushree B Luke, and Ernest Barreto. Networks of theta neurons with time-varying excitability: Macroscopic chaos, multistability, and final-state uncertainty. *Physica D: Nonlinear Phenomena*, 267:16–26, 2014.

[57] S.H. Strogatz. From Kuramoto to Crawford: exploring the onset of synchronization in populations of coupled oscillators. *Physica D*, 143(1-4):1–20, 2000.

[58] Laurette S. Tuckerman and Dwight Barkley. Bifurcation analysis of the eckhaus instability. *Physica D: Nonlinear Phenomena*, 46(1):57 – 86, 1990.

[59] D.A. Wiley, S.H. Strogatz, and M. Girvan. The size of the sync basin. *Chaos: An Interdisciplinary Journal of Nonlinear Science*, 16(1):015103–015103, 2006.

[60] M. Wolfrum, O. E. Omel'chenko, S. Yanchuk, and Y. L. Maistrenko. Spectral properties of chimera states. *Chaos*, 21(1):013112, 2011.

[61] Xiaohui Xie and Martin A Giese. Nonlinear dynamics of direction-selective recurrent neural media. *Physical Review E*, 65(5):051904, 2002.

[62] M. K. Stephen Yeung and Steven H. Strogatz. Time delay in the kuramoto model of coupled oscillators. *Phys. Rev. Lett.*, 82:648–651, Jan 1999.

[63] Damián H Zanette. Propagating structures in globally coupled systems with time delays. *Physical Review E*, 62(3):3167, 2000.